

## Probabilistic evaluation of dynamic positioning operability with a Quasi-Monte Carlo approach



Francesco Mauro<sup>1</sup>, Radoslav Nabergoj<sup>2\*</sup>

<sup>1</sup> Sharjah Maritime Academy, Sharjah, United Arab Emirates

<sup>2</sup> NASDIS PDS d.o.o., Izola, Slovenia

### ARTICLE INFO

Editor-in-Chief: Prof. Nastia Degiuli  
Associate Editor: PhD Ivana Martić  
Dynamic Positioning  
Offshore  
Quasi-Monte Carlo  
Operability

### ABSTRACT

During the design phase of an offshore unit, estimating the station-keeping capabilities of the dynamic positioning (DP) system is mandatory. This means, in conventional offshore applications, to determine the maximum sustainable wind speed as a function of the encounter heading, which the unit may counteract by employing the onboard actuators or mooring lines only. Besides the deterministic estimation of DP capability, it is possible to assess the operability of the DP system following a non-deterministic probabilistic process by employing the site-specific joint wind-wave distributions to model the environment. In such a case, the operability results from a Monte Carlo integration process. Here it is proposed to enhance the applicability of the probabilistic analysis of DP operability, investigating the application of a Quasi-Monte Carlo method. In this sense, the procedure uses quasi-random samplings following a Sobol sequence instead of employing random samples of the joint distributions. In this paper, the Quasi-Monte Carlo process is tested and compared on a reference ship, highlighting the improvements to the established probabilistic DP prediction concerning the number of calculations needed to estimate operability. The significant reduction of computational time makes the newly implemented method suitable for the early design stage applications.

### 1. Introduction

Nowadays, offshore vessels/units operate in open waters characterised by severe weather conditions. Therefore, evaluating the vessel's operability is essential already from the early stages of the design process [1-6]. Operability is a performance indicator that includes her station-keeping capability (Dynamic Positioning operability) and her compliance with recommended motion criteria (seakeeping operability) related to the workability of the crew and specific onboard systems/instrumentations [7,8]. Furthermore, traditional workability criteria are associated with motions and accelerations due to first-order wave forces. In the case of DP, instead, second-order wave drift forces are predominant, together with wind and current loads.

DP is a peculiar system mounted onboard offshore units. Such a system allows the vessel to keep a given position and heading by employing the onboard actuators only. The conventional way to assess the performance of the DP system consists in predicting its capability [9,10].

\* Corresponding author.

E-mail address: [radoslav.nabergoj@nasdispds.com](mailto:radoslav.nabergoj@nasdispds.com)

The present paper deals with determining vessel's station-keeping capability and the proposal of a novel methodology for estimating her DP operability already in the early design stage. The conventional methods for DP predictions consider the quasi-static equilibrium with external loads and delivered thrust to assess the maximum wind speed the DP system can counteract at each encounter angle. Calculations are performed considering all the loads (wind, wave and current) collinear and reported in dedicated diagrams called capability plots [9]. The assessment can be performed through quasi-static analyses [11-13] or dynamic simulations [14,15]. In both cases, the final outcome is a capability plot [9] showing the maximum sustainable wind speed at each heading angle for a set of predetermined environmental conditions [9,10], and, for preliminary calculations, quasi-static analysis is preferred [10]. This is the state-of-the-art method to estimate DP capability in an early design stage. Such an approach implies adopting a wind-wave correlation, which does not properly describe the on-site irregular sea environment. To this end, determining DP operability requires adopting a scatter diagram approach [8] or a multivariate probabilistic definition of the environmental forces [16].

The latter is a probabilistic method, which requires evaluating DP operability through a Monte Carlo (MC) integration process [17]. In this context, determining the station-keeping capability necessitates the execution of multiple repetitions to establish the final value, as MC integration follows a pseudo-random procedure. However, the execution of an MC simulation requires computing a significantly high number of DP calculations [16], which is not beneficial for the early design stage of an offshore unit. In order to achieve a faster calculation method, without losing the added value provided by MC simulation, an alternative approach is required.

To this end, the present study presents an enhancement to the MC process by substituting the MC integration with a Quasi-Monte Carlo (QMC) procedure. Thanks to an algorithm based on a Sobol sequence [18], the integration can be performed in a single calculation without needing multiple repetitions, thus saving significant computational effort. Furthermore, the calculation ensures more even coverage of the calculation space especially when a low number of samples is used, allowing also for the repeatability of the obtained results. The new QMC procedure is then compared to the MC one on a reference offshore vessel, highlighting the benefits in terms of calculations needed for estimating the DP operability.

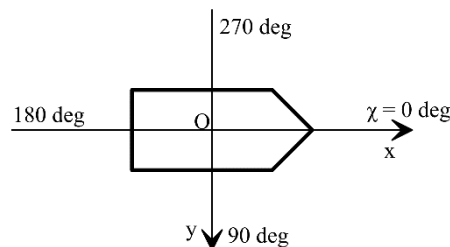


**Fig. 1** Reference system for DP analysis.

## 2. DP analysis

Two different methodologies can evaluate the station-keeping ability of an offshore unit: time domain simulations [14,19] and quasi-static analyses [20,21]. The first method is more time-consuming and is preferable for an advanced design stage when the knowledge of the final thruster layout and the controller is available. The quasi-static approach presents the best suitable option for estimating DP capabilities during the early design stage or for non-definitive thruster configurations. For such reasons, the quasi-static DP capability predictions are the standard approach to DP for the design of offshore units.

The quasi-static approach solves the equilibrium of the forces and moments acting on the offshore unit in the horizontal plane. The method is quasi-static because it includes dynamic effects through empirical allowance coefficients on the environmental loads. Considering a body-fixed reference system centred on the unit's mid-point (see Figure 1), the equilibrium assumes the following form:

$$\mathbf{A}(\boldsymbol{\alpha})\mathbf{f}\mathbf{a} = \mathbf{f}_{\text{ext}} \quad (1)$$

where  $\mathbf{f}_{\text{ext}}=[X_{\text{ext}}, Y_{\text{ext}}, N_{\text{ext}}]^T$  is the external loads vector,  $\mathbf{f}\mathbf{a}=[fa_1, \dots, fa_{Na}]^T$  is the vector of the forces delivered by the  $Na$  onboard actuators and  $\mathbf{A}(\boldsymbol{\alpha})$  in  $\mathbb{R}^{3 \times Na}$  is a matrix whose elements contain the actuator positions and the actuator forces orientations  $\boldsymbol{\alpha}=[\alpha_1, \dots, \alpha_{Na}]^T$ .  $\mathbf{A}(\boldsymbol{\alpha})$  matrix is specific for each offshore unit, as it depends on the type and position of the onboard actuators. Matrix  $\mathbf{A}(\boldsymbol{\alpha})$  is formed from a set of  $Na$  column vectors  $\mathbf{a}_i$  in  $\mathbb{R}^3$  having different forms according to the onboard actuator's type. The following formulations apply to the most commonly used actuator types for DP operations:

$$\mathbf{a}_i = \begin{cases} [1, 0, -r_{yi}]^T & \text{main propellers} \\ [0, 1, r_{xi}]^T & \text{fixed tunnel thrusters or rudders} \\ [\cos \alpha_i, \sin \alpha_i, r_{xi} \sin \alpha_i - r_{yi} \cos \alpha_i]^T & \text{azimuth thrusters} \end{cases} \quad (2)$$

where  $r_{xi}$  and  $r_{yi}$  are the longitudinal and transversal coordinates of the location of the onboard actuators.

The unknowns of the system (1) are the actuator forces  $\mathbf{f}\mathbf{a}$  and the orientations  $\boldsymbol{\alpha}$ . The number of unknowns  $Nu$  depends on the actuator's type. Generally, azimuth thrusters have two unknowns (thrust and orientation), while rudders, propellers and tunnel thrusters have one unknown only (the thrust or the orientation). Therefore, as a general rule, the number of unknowns is  $Nu=Na+Nat$ , where  $Nat$  is the number of azimuth thrusters installed onboard the offshore unit. It can be convenient to incorporate the unknowns in a vector  $\mathbf{u}=[\mathbf{f}\mathbf{a}, \boldsymbol{\alpha}]^T$  in  $\mathbb{R}^{Nu}$ . Matrix  $\mathbf{A}(\boldsymbol{\alpha})$  has rank 3 and vector  $\mathbf{u}$  has rank  $Nu$ . Therefore, system (1) admits a unique solution only in the case of  $Nu=3$ . Such a condition is practically unrealistic as it can be achieved by configurations having one azimuth thruster and a tunnel thruster or three tunnel thrusters. Both these examples are not suitable for DP operations.

Conventional DP configurations always have  $Nu>3$ ; thus, system (1) admits infinite solutions. Therefore, the resolution of the quasi-static DP requires adopting an alternative resolution method.

## 2.1 Thrust allocation

The most suitable technique to solve the quasi-static equilibrium system for DP purposes is to consider a constrained optimisation problem. Such a strategy allows for determining  $\mathbf{u}$ , which means the forces  $\mathbf{f}\mathbf{a}$  and the orientations  $\boldsymbol{\alpha}$ , minimising an approximating function of the power absorbed by the DP system in a given condition. The objective function has the following form [17]:

$$\min(z) = \sum_{i=1}^{Na} |fa_i|^{3/2} \quad (3)$$

The objective function is subject to the following constraints [17]:

$$\mathbf{A}(\boldsymbol{\alpha})\mathbf{f}\mathbf{a} = \mathbf{f}_{\text{ext}} \quad (4)$$

$$\mathbf{f}\mathbf{a}_{\min} \leq \mathbf{f}\mathbf{a} \leq \mathbf{f}\mathbf{a}_{\max} \quad (5)$$

$$\boldsymbol{\alpha}_{\min} \leq \boldsymbol{\alpha} \leq \boldsymbol{\alpha}_{\max} \quad (6)$$

Equation (4) represents the static equilibrium of the forces as per system (1), equation (5) allows for allocating thrust only between the actuator saturation limits and equation (6) identifies the feasible sectors for the angles  $\alpha_i$ .

The problem described by equation (3) with the constraints given by equations (4), (5) and (6) is non-linear and non-convex, and is solvable through a non-linear iterative optimization algorithm [22]. Such a method can handle the thrust allocation problem considering unknowns  $\mathbf{f}\mathbf{a}$  and  $\boldsymbol{\alpha}$  or considering the thrust components  $\mathbf{f}\mathbf{a}_x = \mathbf{f}\mathbf{a} \cos \boldsymbol{\alpha}$  and  $\mathbf{f}\mathbf{a}_y = \mathbf{f}\mathbf{a} \sin \boldsymbol{\alpha}$ , expressed in the body-fixed reference system [23]. The change of

variables maintains the non-linearity of the objective function. However, constraint (4) becomes linear, and equation (5) can be linearised by adding additional inequality linear constraints without losing the accuracy of the final result. Finally, the feasible region of the azimuth angles  $\alpha$  is substituted by automatically adding equality constraints to the problem, forcing the solution to be in the feasible region border when needed. As a result, the thrust allocation algorithm determines, besides the specific thrust intensity and orientation of the actuators, whether the DP system is capable of keeping position, thus respecting the equilibrium request of equation (1).

## 2.2 Environmental loads modelling

According to the definition of DP and equation (1), the actuator's forces  $\mathbf{fa}$  should counteract the external forces  $\mathbf{fext}$ . The external forces include different kinds of loads, according to the operation of the offshore unit. A general decomposition of  $\mathbf{fext}$  is as follows:

$$\mathbf{fext} = \mathbf{fenv} + \mathbf{fop} \quad (7)$$

where  $\mathbf{fenv}=[X_{env},Y_{env},N_{env}]^T$  is the vector of the environmental forces and  $\mathbf{fop}=[X_{op},Y_{op},N_{op}]^T$  is the vector of the additional external forces depending on the unit operations, i.e. pipe laying [24,25], lifting, assisted mooring [26], etc.

The additional operational loads  $\mathbf{fop}$  are not always present in a DP analysis; thus, the most relevant part of the external loads  $\mathbf{fext}$  are the environmental loads  $\mathbf{fenv}$ . These loads are composed of several forces that may act on the unit during an operation in open seas. Conventionally, the environmental loads have the following breakdown:

$$\mathbf{fenv} = (\mathbf{f}_{wind} + \mathbf{f}_{wave} + \mathbf{f}_{curr}) CA_{dyn} \quad (8)$$

where  $\mathbf{f}_{wind}=[X_{wind},Y_{wind},N_{wind}]^T$  is the wind loads vector,  $\mathbf{f}_{wave}=[X_{wave},Y_{wave},N_{wave}]^T$  is the wave loads vector and  $\mathbf{f}_{curr}=[X_{curr},Y_{curr},N_{curr}]^T$  is the current loads vector. The last term in equation (8) is the dynamic allowance  $CA_{dyn}$ , an empirical coefficient incorporating dynamics effects on the static loads. The coefficient can be derived from time-domain simulations on similar offshore units or using recommendations given by Classification Societies. In the present study, a  $CA_{dyn}=1.25$  is used, as suggested by DNV-GL [10].

The conventional way to evaluate the environmental loads employs non-dimensional coefficients expressed as a function of the heading angle  $\chi$ . This approach allows for using coefficients of similar ships instead of performing model tests or complex calculations for each new unit [11]. For wind and current loads, the following formulations are valid [16]:

$$\mathbf{f}_{wind} = \begin{bmatrix} X_{wind} \\ Y_{wind} \\ N_{wind} \end{bmatrix} = \frac{1}{2} \rho_{air} V_w^2 \begin{bmatrix} A_T \\ A_L \\ A_L L_{OA} \end{bmatrix} \mathbf{C}_{wind}(\chi) \quad (9)$$

$$\mathbf{f}_{curr} = \begin{bmatrix} X_{curr} \\ Y_{curr} \\ N_{curr} \end{bmatrix} = \frac{1}{2} \rho_{water} V_c^2 \begin{bmatrix} S \\ S \\ SL_{WL} \end{bmatrix} \mathbf{C}_{curr}(\chi) \quad (10)$$

where  $\rho_{air}$  is the air density,  $\rho_{water}$  is the water density,  $V_w$  is the wind speed,  $V_c$  is the underwater current speed,  $A_T$  is the transversal area exposed to wind,  $A_L$  is the lateral area exposed to wind,  $S$  is the wetted surface,  $L_{OA}$  is the overall length and  $L_{WL}$  is the waterline length of the offshore unit. The other quantities in equations (9) and (10) are the non-dimensional wind coefficients  $\mathbf{C}_{wind}=[C_{Xw},C_{Yw},C_{Nw}]^T$  and the non-dimensional current coefficients  $\mathbf{C}_{curr}=[C_{Xc},C_{Yc},C_{Nc}]^T$ , both functions of the heading angle  $\chi$ .

Quite different is the case of wave forces, which, for DP purposes, requires the modelling of the mean drift components. The sea states refer to an irregular long-crested wave environment described by specific

couples of significant wave heights  $H_s$  and zero crossing periods  $T_z$ . The mean drift forces derive from model experiments or diffraction calculations, providing the quadratic transfer functions (QTFs) necessary to evaluate the loads in different sea states. Therefore, modelling the irregular waves through a spectrum with specific  $H_s$  and  $T_z$ , the drift forces result from the following expressions [16]:

$$\mathbf{f}_{\text{wave}} = \begin{bmatrix} X_{\text{wave}} \\ Y_{\text{wave}} \\ N_{\text{wave}} \end{bmatrix} = g \rho_{\text{water}} \begin{bmatrix} \nabla^{1/3} \\ \nabla^{1/3} \\ \nabla^{2/3} \end{bmatrix} \int_0^\infty \mathbf{C}_{\text{wave}}(\chi, \omega) S_\zeta(\omega) d\omega \quad (11)$$

where  $g$  is the acceleration of gravity,  $\nabla$  is the vessel's volume,  $S_\zeta$  is the wave amplitude spectrum expressed as a function of the circular wave frequency  $\omega$  and  $\mathbf{C}_{\text{wave}} = [C_{X\text{wave}}, C_{Y\text{wave}}, C_{N\text{wave}}]^T$  is the QTFs vector expressed as a function of frequency  $\omega$  and heading  $\chi$ .

Alternative simplified methodologies for load determination can be applied as suggested by IMCA [9]. In the present study, no particular effort has been dedicated to environmental loads modelling and, therefore, simplified formulations have been used [9,10].

The proposed modelling requires defining a tuple of parameters  $\mathbf{e} = [V_W, V_c, H_s, T_z, \chi]^T$  to set up the optimisation problem. Furthermore, as an assumption, the loads are supposed to be concurrent. Another simplification for quasi-static DP predictions concerns the current velocity, usually set constant through all the environmental conditions [9]. Here  $V_c = 0.75$  m/s is considered for all the tested cases [10]. The DP capability calculations are performed with the aid of implemented and self-developed code by the authors.

### 2.3 DP operability

The conventional approach to quasi-static DP predictions considers fixed empirical relationships between wind speed and wave parameters, providing the maximum sustainable wind speed as a function of the heading angle  $\chi$ . This approach determines the DP capability through polar plots obtained by monotonically increasing the wind speed  $V_W$ . However, this method considers only a few deterministic sea state conditions, which do not represent all the environmental conditions the unit may encounter during operations. Therefore, an alternative approach to quasi-static DP is necessary to simulate a realistic sea environment with all the feasible conditions properly accounted for.

A suitable alternative is the scatter diagram approach [8]. Instead of performing DP calculations for fixed combinations of wind and waves, the methodology covers all the cells of a scatter diagram, which means calculating the quasi-static equilibrium for all the couples of  $H_s$  and  $T_z$  representative of a sea area. Calculations consider each single heading angle  $\chi$  and allow for a novel approach for DP performance predictions, evaluating no more the deterministic station-keeping capability but the semi-probabilistic DP operability for the selected geographic area with given  $H_s$  and  $T_z$  distribution and unknown wind speed correlation. In this case, DP operability has the following formulation [8]:

$$OP_{DP} = \sum_{i=1}^{N_\chi} f_{\chi i} \sum_{j=1}^{NH_s} \sum_{k=1}^{NT_z} f_{\text{wjk}} I_{DPijk} \quad (12)$$

where  $\mathbf{f}_\chi = [f_{\chi 1}, \dots, f_{\chi N_\chi}]^T$  in  $\mathbb{R}^{N_\chi}$  is the vector of the occurrence of the  $N_\chi$  headings and  $\mathbf{f}_w = [f_{w11}, \dots, f_{w1NT_z}; \dots, f_{wNH_s1}, \dots, f_{wNH_sNT_z}]$  in  $\mathbb{R}^{NH_s \times NT_z}$  is the matrix describing the joint occurrence of  $H_s$  and  $T_z$  given by a scatter diagram with granularity  $NH_s$  for the wave heights and  $NT_z$  for the wave periods. The last term in equation (12) is the matrix  $\mathbf{IDP}$  in  $\mathbb{R}^{N_\chi \times NH_s \times NT_z}$ , which represents the results of the quasi-static calculation. As such, the members of  $\mathbf{IDP}$  are equal to 1 in case a feasible solution exists for the optimisation problem of equation (3) and 0 otherwise. That means the value of 1 indicates that the DP system holds the position.

However, a scatter diagram covers only a combination of wave parameters ( $H_s$  and  $T_z$ ), without giving information on the wind speed  $V_W$ . Being equation (12) discrete, it is convenient to consider a single value of  $V_W$  per each couple ( $H_s, T_z$ ) adopting a deterministic and simplified procedure derived from the Pierson-

Moskowitz wave spectrum [3]. This simplified approach allows for the evaluation of  $OP_{DP}$  in every worldwide operational area but without considering the proper statistic for  $V_W$  in the selected sea area.

### 3. Operability as a Quasi-Monte Carlo process

The DP operability following a scatter diagram approach [8] is limited by not considering proper modelling for the wind statistics in a reference sea area. An enhancement to the scatter diagram approach is considering the environmental modelling with continuous multivariate probabilistic distributions. Adopting a continuous model for the environmental loads' definition implies the calculation of operability with a continuous formulation through a Monte Carlo (MC) integration [17].

The random nature of the MC process requires the execution of multiple runs of  $OP_{DP}$  calculations to determine a mean value and an associated confidence interval, significantly increasing the computational effort. The early design stage needs methodologies that are fast and sufficiently reliable; therefore, finding a method that reduces the computational needs for DP evaluation is a meaningful enhancement. To this end, a Quasi-Monte Carlo (QMC) approach can substitute the MC process, decreasing the computational effort. Hereafter, the section describes the main peculiarities of the multivariate modelling and the QMC integration process to determine DP operability.

#### 3.1 Tri-variate wind-wave modelling

A substantial change in modelling the long-term area-specific environmental conditions could enhance the DP operability predictions described by the scatter diagram approach. The use of data, when available, derived from local measurements or weather forecasting models allows for modelling the environmental conditions through joint wind-wave probabilistic distributions. More precisely, having the necessity of describing the mutual behaviours of  $V_W$ ,  $H_s$  and  $T_z$ , there is a need to define a tri-variate joint distribution. The modelling adopted in the study considers the peak period  $T_p$  instead of the  $T_z$  employed by the scatter diagrams; however, the relationship between the two periods is straightforward according to the adopted irregular wave spectrum [16].

Stating the above, a suitable joint distribution for  $V_W$ ,  $H_s$  and  $T_p$  is as follows [16]:

$$f_{V_W H_s T_p}(v_w, h_s, t_p) = f_{V_W}(v_w) f_{H_s|V_W}(h_s, v_w) f_{T_p|V_W H_s}(v_w, h_s, t_p) \quad (13)$$

where  $v_w$ ,  $h_s$  and  $t_p$  are three aleatory variables in  $(0, +\infty)$  needed to define the joint distribution. Equation (13) incorporates a marginal distribution  $f_{V_W}$  for the wind speed, a conditional distribution  $f_{H_s|V_W}$  for the wave height and another conditional distribution  $f_{T_p|V_W H_s}$  for the wave period. The distributions have the following form [16]:

$$f_{V_W}(v_w) = \frac{\beta_v}{\eta_v} \left( \frac{v_w}{\eta_v} \right)^{\beta_v - 1} \exp\left(-\left(\frac{v_w}{\eta_v}\right)^{\beta_v}\right) \quad (14)$$

$$f_{H_s|V_W}(h_s, v_w) = \frac{\beta_h(v_w)}{\eta_h(v_w)} \left( \frac{h_s}{\eta_h(v_w)} \right)^{\beta_h(v_w) - 1} \exp\left(-\left(\frac{h_s}{\eta_h(v_w)}\right)^{\beta_h(v_w)}\right) \quad (15)$$

$$f_{T_p|V_W H_s}(v_w, h_s, t_p) = \frac{1}{\sqrt{2}\sigma_{T_p}(h_s)t_p} \exp\left[-\frac{1}{2}\left(\frac{\ln t_p - \mu_{T_p}(v_w, h_s)}{\sigma_{T_p}(h_s)}\right)^2\right] \quad (16)$$

Equations (14) and (15) are two-parameters Weibull distributions, while equation (16) is a log-normal distribution. A detailed description of the parameters of the above equations is given in [16,17]. Parameters are site-specific and derived from fitting procedures on environmental data.

This kind of modelling for the environmental loads does not allow anymore a univocal combination of  $H_s$ ,  $T_z$  and  $V_W$  necessary to evaluate  $OP_{DP}$  through the scatter diagram approach of equation (12).

### 3.2 Quasi-Monte Carlo Integration

The tri-variate modelling for the environmental condition forces a change in the formulation of the DP operability. As mentioned above, the scatter diagram approach is no longer applicable, but the problem becomes a multi-dimensional MC integration [17]. A general MC integral has the following form:

$$\int_{\Omega} f(\mathbf{x}) d\mathbf{x} \approx \frac{1}{N_s} \int_{\Omega} d\mathbf{x} \sum_{i=1}^{N_s} f(\mathbf{x}_i) \quad (17)$$

where  $\Omega$  in  $\mathbb{R}^m$  is an  $m$ -dimensional probability space,  $\mathbf{x}$  in  $\Omega$  is a matrix of  $m$  independent random variables having  $N_s$  element each. Equation (17) becomes simpler in case  $\Omega$  is a unit-hypercube  $(0,1)^m$ , which means the integral  $\int_{\Omega} d\mathbf{x}$  is 1. Then, considering a set of  $m$  uniform random variables  $\mathbf{U} \sim \mathbf{U}(0,1)$ , the integral assumes the following form:

$$\int_{\Omega} f(\mathbf{x}) d\mathbf{x} \approx \frac{1}{N_s} \sum_{i=1}^{N_s} f(\mathbf{U}_i) \quad (18)$$

Considering the tri-variate joint distribution of equation (13) and modelling the heading angle as a uniform random variable, equation (12) can be adapted to an MC process as follows:

$$OP_{DP} = \frac{1}{N_s} \sum_{i=1}^{N_s} f_{\chi}(\mathbf{U}_{\chi}) f_{V_W H_s T_p}(\mathbf{U}_{v_w}, \mathbf{U}_{h_s}, \mathbf{U}_{t_p}) I_{DP_i} \quad (19)$$

where  $f_{\chi}$  is the function of the headings, independent from  $V_W$ ,  $H_s$  and  $T_p$ . According to equation (19), it is sufficient to generate a tuple  $\mathbf{e}^* = [\chi, V_W, H_s, T_p]^T$  to evaluate the operability. The process of a crude MC integral generates the tuple from a direct sampling in  $\mathbf{U}$  through pseudo-random numbers [27]. However, the use of pseudo-random numbers introduces uncertainties in the calculation of the integral, as the approximated integral converges to an exact value as  $N_s$  increases without upper bounds. It is then necessary to use a sufficiently large number of samples that ensures the matching of the required confidence level for the solution. This can be achieved by calculating a Confidence Interval (CI) across multiple repetitions  $N_r$  [17].

An alternative sampling strategy, aimed to reduce the variance of a crude MC integration, is the adoption of Quasi-random methods [28]. Thanks to the use of low-discrepancy sequences it is possible to achieve lower errors than crude MC on practical integration problems. Between the different deterministic low-discrepancy sequences, the Sobol chain presents an attractive option, giving a good reproduction of the uniform distribution even with low sample size and without high computational effort [18]. Figure 2 shows the differences between crude MC and QMC with Sobol sequences for the sampling of a bivariate uniform distribution with  $10^3$  samples. This example highlights the differences in the coverage of a sampling space given by the two procedures. QMC method grants a more uniform coverage with a lower number of samples, avoiding agglomeration of points and void spaces typical of a crude MC approach.

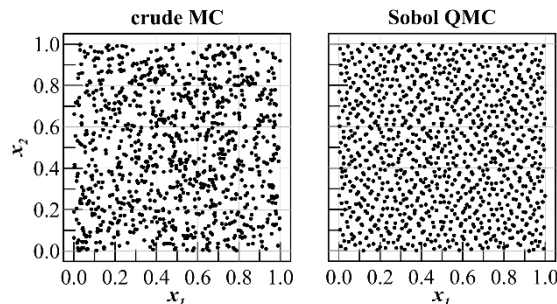


**Fig. 2** Bi-dimensional uniform distribution according to crude MC and Sobol QMC ( $N_s=10^3$ )

Following a QMC approach, the generation of  $\mathbf{e}^*$  with a sample size  $N_s=10^5$  follows the subsequent steps:

1. Generation of  $\mathbf{\Omega}=[\mathbf{U}_\chi, \mathbf{U}_{vw}, \mathbf{U}_{Hs}, \mathbf{U}_{Tp}]^T$  with multidimensional Sobol sequences.
2. Direct determination of  $\chi$  from  $\mathbf{U}_\chi$ .
3. Inversion of equation (14) to obtain the wind speed random variable  $v_W$ .
4. Inversion of equation (15) to obtain the significant wave height random variable  $h_s$ .
5. Inversion of equation (16) to obtain the wave period random variable  $t_p$ .
6. Determination of  $\mathbf{e}^*$  for all the  $N_s$  samples.

Applying the above steps, it is possible to generate  $N_s$  samples of the joint environmental characteristics for a specific area and then apply equation (19) to determine DP operability. The QM and QMC methodologies have been included in the in house DP code used for the simulations presented in the case study.

#### 4. Case study

The present study employs as a reference test an offshore supply vessel (OSV), having the main dimensions and actuator configuration reported in Table 1 and Table 2, respectively. The DP system presents four actuators: 2 tunnel thrusters and 2 azimuth thrusters. According to the definition of the unknowns, the reference OSV has  $N_u=6$  and the unknowns vector is  $\mathbf{u}=[fa_1, fa_2, fa_3, fa_4, \alpha_3, \alpha_4]^T$  in  $\mathbb{R}^6$ . Figure 3 shows the actuator configuration of the reference OSV.

**Table 1** Reference OSV main characteristics

Name	Symbol	Value	Unit
Length between perpendiculars	$L_{PP}$	72.00	m
Length overall	$L_{OA}$	78.35	m
Maximum breadth	$B$	16.00	m
Operative draught	$T$	4.05	m
Volume	$\nabla$	3245.21	$\text{m}^3$
Lateral exposed wind area	$A_L$	854.10	$\text{m}^2$
Transversal exposed wind area	$A_T$	187.40	$\text{m}^2$

**Table 2** Reference OSV actuator configuration.

Actuator ID and type	$r_x$ (m)	$r_y$ (m)	$F_{amax}$ (kN)
A1 (tunnel thruster)	32.00	0.00	73.50
A2 (tunnel thruster)	-30.00	0.00	62.50
A3 (azimuth thruster)	-36.00	-3.00	240.00
A4 (azimuth thruster)	-36.00	-3.00	240.00

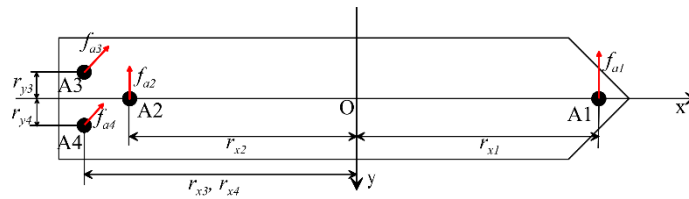


**Fig. 3** Actuators configuration for the reference OSV.

The reference OSV is supposed to operate in five different sea areas, already defined with the tri-variate joint distributions for the environmental loads in [17]. The previous study shows the result of applying the crude MC integration to evaluate  $OP_{DP}$  in the five areas. Here, the application of the QMC integration is



presented and compared to the MC results. According to the described procedure, the first step consists of performing the QMC sampling of the uniform distribution to determine  $\mathbf{e}^*$  on the space  $\Omega$ . Afterwards, the procedure continues with the execution of quasi-static DP calculations for each of the  $N_s$  samples. The present study considers  $N_s=10^5$  in accordance with the previous analysis with MC integration. The main difference is in the number of repetitions, as the QMC process needs only one process while for MC analysis 10 repetitions were used to evaluate a CI on the mean  $OP_{DP}$  value.

Figure 4 shows the results of the DP analysis with the QMC method on the  $H_s$ - $T_p$  plane, compared to the MC approach. The figure compares the values for  $I_{DP}$  obtained in the five operational areas. It can be noticed that the QMC sampling covers more evenly the probability space of the environmental conditions identifying a more dense area where the DP system is not capable of holding the position.

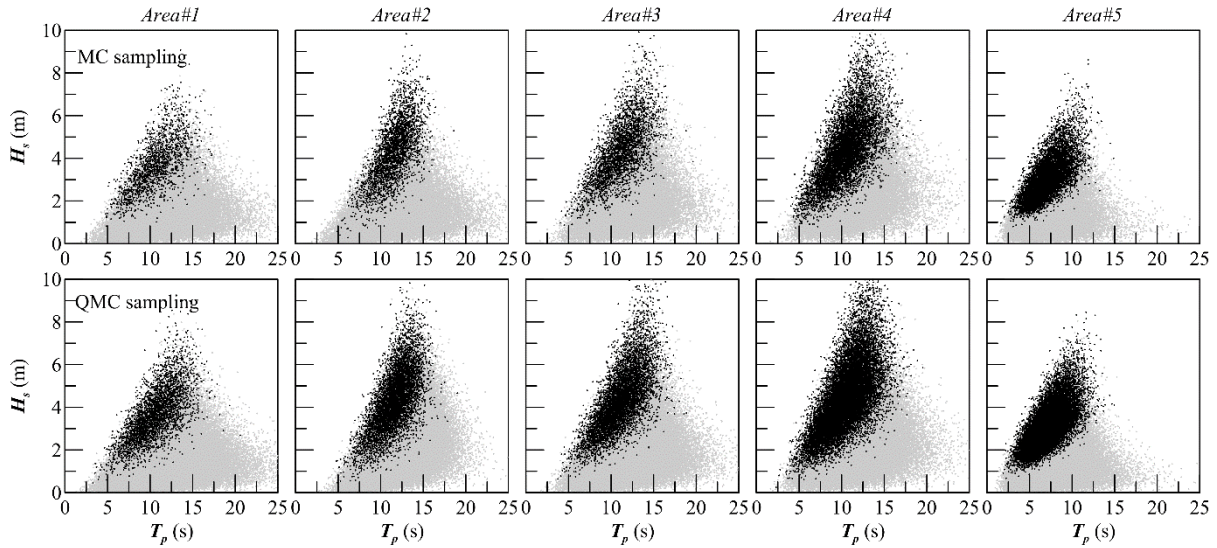


**Fig. 4**  $I_{DP}$  values (grey for  $I_{DP}=0$ , black for  $I_{DP}=1$ ) as a function of  $H_s$  and  $T_p$  according to MC (top) and QMC (bottom) sampling.

Another important issue is the integral convergence. Figure 5 shows the convergence history, monitoring the relative differences between  $OP_{DP}$  values at consecutive integration steps:

$$\Delta OP_{DP} = \left| \sum_{j=1}^i \frac{I_{DP_j}}{i} - \sum_{j=1}^{i-1} \frac{I_{DP_j}}{j-1} \right| \quad (20)$$

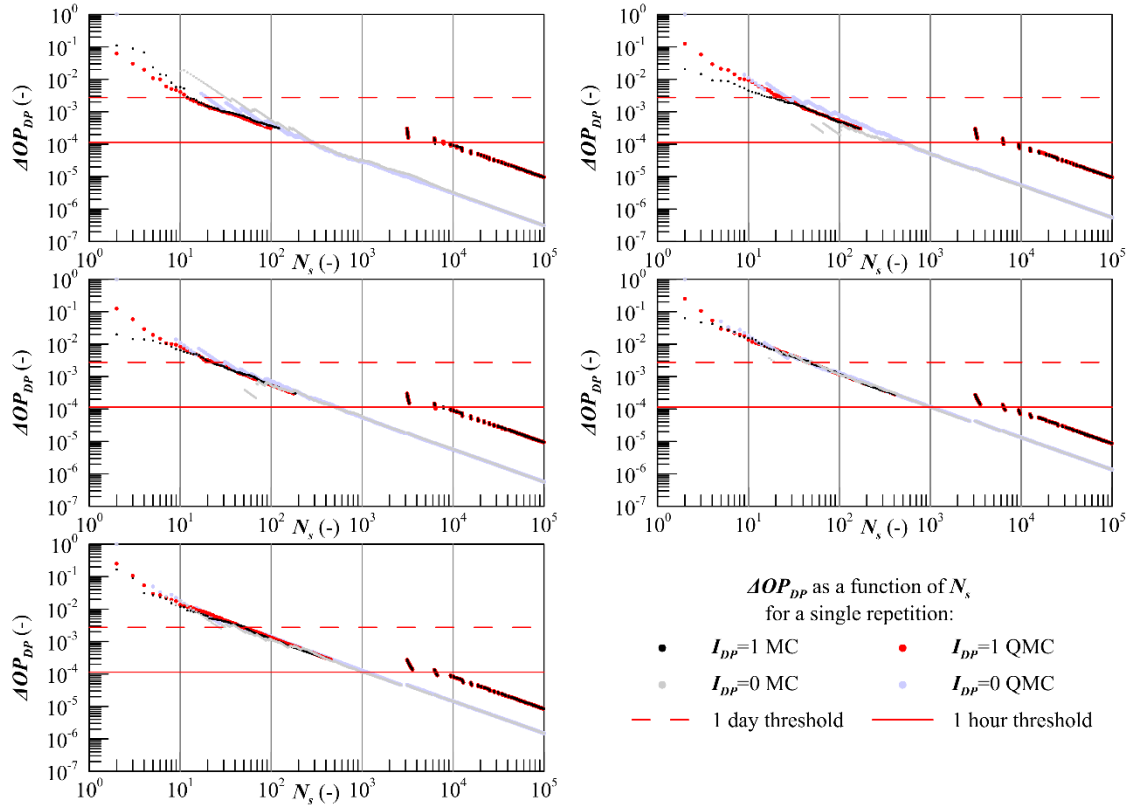


**Fig.5** Comparing convergence of MC and QMC processes for the five reference sea areas.

The values for  $\Delta OP_{DP}$  are compared with two reference thresholds, representative of 1 day of operability (corresponding to an  $OP_{DP}=2.74 \cdot 10^{-3}$ ) and 1 hour (corresponding to an  $OP_{DP}=1.144 \cdot 10^{-4}$ ). As  $I_{DP}$ , the integrating function, has only two possible discrete values, the  $\Delta OP_{DP}$  curve has two distinct trends and, consequently, the convergence should be checked on the higher sequence of points (the one corresponding to  $I_{DP}=1$ ) in the reference  $N_s$  range.

Figure 4 contains also the value obtained with the MC integration for one of the 10 repetitions. From the figure, it is not possible to clearly distinguish between the convergence process of the MC and QMC integral. It can be observed that for the 5 areas, the 1-day threshold is reached with less than 100 samples while satisfying the 1-hour threshold requires almost  $10^4$  samples for all the tested cases. This is valid for both integration strategies.

However, considering only one repetition is misleading for the MC process and an effective comparison can be made only considering all the ten repetitions, providing the confidence interval on the mean.

Therefore, Figure 6 shows the solution history of the  $OP_{DP}$  for the  $N_r=10$  MC integration together with the single repetition of the QMC approach. The figure reports a confidence interval obtained from the following formulation:

$$CI(c) = \mu \pm t \frac{\sigma}{N_r} \tag{21}$$

where  $\mu$  is the  $OP_{DP}$  mean of the  $N_r$  repetitions,  $\sigma$  is the  $OP_{DP}$  variance,  $t$  is the inverse of the cumulative density function of the Student-t distribution with confidence interval  $c$  and  $N_r$  degrees of freedom. In the applied example, a 95% CI has been considered.

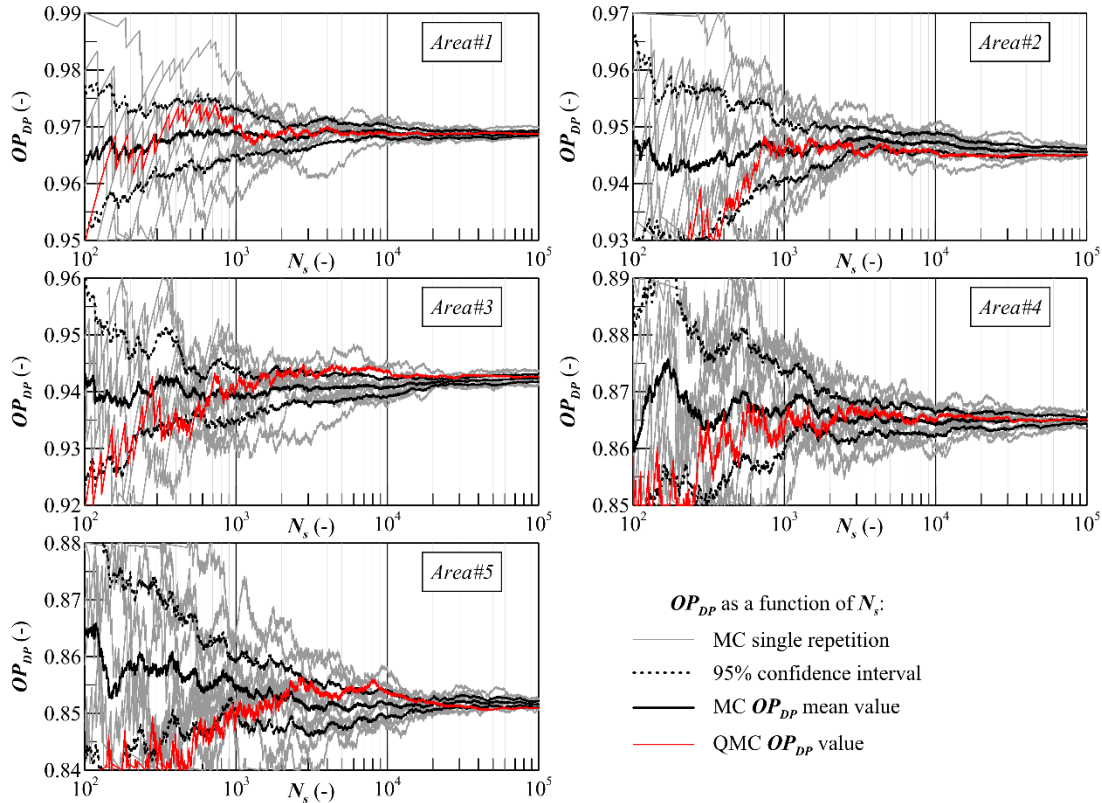


Fig. 6 Solution history of  $OP_{DP}$  in five selected areas according to QMC approach and MC approach with  $N_r=10$ .

As already observed in the previous study, the CI is always higher than the 1-hour threshold also for  $N_s=10^5$ , highlighting the variability of a fully random process as the crude MC integration. Analysing the QMC results, it is possible to observe that for all the five reference areas, the integral lies between the CI of the MC integration for  $N_s > 10^3$ , which, according to MC analysis, is sufficient to grant the 1-day threshold in almost all the reference sea areas. In any case, the final values of the integration do not change, as  $N_s=10^5$  is sufficiently high to ensure the convergence of both processes. However, considering lower values for  $N_s$  highlights differences in the  $OP_{DP}$  evaluated with the QMC method. Differences that remain inside the CI of the MC process are thus not significant from an engineering point of view.

Therefore, the adoption of a QMC integration allows for significantly reducing the total computational effort to determine the operability of a DP system for different sea areas. In fact, the novel approach allows for saving 10 times the calculation time compared to the MC approach, which is a considerable improvement for early-design stage applications. Furthermore, the QMC method allows for an increase in the reliability of the prediction with a low number of samples, ensuring more even coverage of the calculation space and the reproducibility of the final results, something non-achievable by a crude MC integration.

## 5. Conclusions

The present work implements a methodology based on QMC integration to perform area-specific DP predictions, starting from the modelling of environmental parameters with joint tri-variate distributions. The process is an enhancement of a methodology developed by employing a crude MC method to estimate the DP operability in different sea areas. The advantage of the QMC method compared to MC integration lies in the possibility of performing a single repetition of calculation, thanks to the adoption of deterministic Sobol sequences for the sampling process instead of using pseudo-random numbers. The application of the process to a reference OSV allows a comparison of the two methodologies, showing no differences in the convergence of a single calculation. However, once all the repetitions of the MC process are compared to the QMC results it is evident that the QMC integration remains inside the confidence interval of the MC process for  $N_s > 10^3$ . The application of QMC methodology is more complicated than crude MC integration as it requires the implementation of the Sobol quasi-random sequence. However, the reduction in computational time and

repetition number is significant and withstands the implementation difficulties. Another limitation concerns the availability of tri-variate environmental data at site. However, programs of weather forecasting, actually employed by offshore operators, could produce suitable sets of local data.

For such a reason the QMC integration is a reliable methodology to perform DP operability analysis for site-specific conditions saving computational time compared to MC integration. This aspect is crucial for the early design stage of an offshore unit, where fast and reliable tools should be employed to estimate the unit's performance and optimum thrusters' selection. Further investigations are needed to establish a physically consistent procedure for DP predictions fully based on probabilistic and site-specific weather conditions instead of deterministic correlations for standard DP capability assessment.

## REFERENCES

- [1] Ghaemi, M.H., Olszewski, H., 2017. Total Ship Operability-Review, Concept and Criteria. *Polish Maritime Research*, 24, 74-81. <https://doi.org/10.1515/pomr-2017-0024>
- [2] Gutsch, M., Steen, S., Sprenger, F., 2020. Operability robustness index as seakeeping performance criterion for offshore vessels. *Ocean Engineering*, 217, 107931. <https://doi.org/10.1016/j.oceaneng.2020.107931>
- [3] Mauro, F., Nabergoj, R., 2020. A global operability index for an offshore vessel. *International Conference on Offshore Mechanics and Arctic Engineering OMAE, Volume 1: Offshore Technology*, 3-7 August, Virtual. <https://doi.org/10.1115/OMAE2020-18650>
- [4] Li, B., Qiao, D. Zhao, W., Hu, Z., Li, S., 2022. Operability analysis of SWATH as a service vessel for offshore wind turbine in southeastern coast of China. *Ocean Engineering*, 251, 111017. <https://doi.org/10.1016/j.oceaneng.2022.111017>
- [5] Calavia, J.R., Paalvast, M., Ledoux, B., Kymmell, J., 2022. Derivation of vessel motion as operational limits and motion forecasting with 2D wave spectra: case study of inter-array subsea cable installation in the North Sea. *International Conference on Offshore Mechanics and Arctic Engineering OMAE, Volume 3: Materials Technology; Pipelines, Risers, and Subsea Systems*, 5-10 June, Hamburg, Germany.
- [6] Sreenivasan, A., Voogt, A., 2022. Numerical Simulations to Determine Comparative Operability of Floating Feeder Solutions. *SNAME Maritime Convention, SMC 2022*, 27-29 September, Houston, Texas, USA. <https://doi.org/10.5957/SMC-2022-033>
- [7] Nabergoj, R., 2011. Station Keeping and Seakeeping in Offshore Vessels Design. *International Symposium on Naval Architecture and Maritime INT-NAM 2011*, 24-25 October, Istanbul, Turkey.
- [8] Mauro, F., Prpić-Oršić, J., 2020. Determination of a DP operability index for an offshore vessel in early design stage. *Ocean Engineering*, 195, 106764. <https://doi.org/10.1016/j.oceaneng.2019.106764>
- [9] IMCA, 2000. IMCA M 140 Rev. I Specification for DP Capability Plots, The International Marine Contractors Association.
- [10] DNV-GL, 2021. DNV-ST-0111 Assessment of station keeping capability of dynamic positioning vessels, Det Norske Veritas, edition December 2021.
- [11] Aalberts, A., Kuipers, R., van Walree, F., Jansen, R., 1995. Developments in Dynamic Positioning systems for offshore stationkeeping and offloading. *The Fifth International Offshore and Polar Engineering Conference*, 11-16 June, The Hague, The Netherlands.
- [12] Wang, I., Yang, J., Xu, S., 2018. Dynamic Positioning capability analysis for marine vessels based on DPCAP polar program. *China Ocean Engineering*, 32, 90-98. <https://doi.org/10.1007/s13344-018-0010-4>
- [13] Prpić-Oršić, J., Valčić, M., 2020. Derivative free optimal thrust allocation in ship dynamic positioning based on direct search algorithms. *TransNav*, 14(2), 309-314. <https://doi.org/10.12716/1001.14.02.05>
- [14] Smogeli, O., Trong, N., Borhaug, B., Pivano, L., 2013. The next level DP capability analysis. *Dynamic Positioning Conference*, 15-16 October, Houston, Texas, USA.
- [15] Martelli, M., Faggioni, N., Donnarumma, S., 2022. A time-domain methodology to assess the dynamic positioning performances. *Ocean Engineering*, 247, 110668. <https://doi.org/10.1016/j.oceaneng.2022.110668>
- [16] Mauro, F., Nabergoj, R., 2022. A probabilistic approach for dynamic positioning capability and operability predictions. *Ocean Engineering*, 262, 112250. <https://doi.org/10.1016/j.oceaneng.2022.112250>
- [17] Nabergoj, R., Mauro, F., 2022. A Monte Carlo Approach for the fully probabilistic evaluation of operability in ship dynamic positioning scenarios. *11<sup>th</sup> International conference on mathematical modelling in physical science*, 5-8 September, Belgrade, Serbia. <https://doi.org/10.1063/5.0163317>
- [18] Sobol, I., Asotky, D., Krenin, A., Kucherenko, S., 2011. Construction and comparison of high-dimensional Sobol' generations. *Wilmott Journal*, 64-73. <https://doi.org/10.1002/wilm.10056>
- [19] Mauro, F., Gaudiano, F., 2018. Station keeping calculations in early design stage: two possible approaches. *Technology and Science for the Ships of the Future*, IOS Press, 372-379.

- [20] Aalberts, A., Kuipers, F., van Walree, F., Jansen, R., 1995. Developments in dynamic positioning systems for offshore stationkeeping and offloading. *ISOPE International Ocean and Polar Engineering Conference*, ISOPE-I.
- [21] Wang, I, Yang, J., Xu, S., 2018. Dynamic Positioning capability analysis for marine vessels based on DPCAP polar program. *China Ocean Engineering*, 32, 90-98. <https://doi.org/10.1007/s13344-018-0010-4>
- [22] Mauro, F., Nabergoj, R., 2016. Advantages and disadvantages of thrust allocation procedures in preliminary dynamic positioning predictions. *Ocean Engineering*, 123, 96-102. <https://doi.org/10.1016/j.oceaneng.2016.06.045>
- [23] Mauro, F., Benci, A., Ferrari, V., Della Valentina, E., 2021. Dynamic Positioning analysis and comfort assessment for the early design stage of large yachts. *International Shipbuilding Progress*, 68, 33-60. <https://doi.org/10.3233/ISP-210508>
- [24] Nabergoj, R., Ardavanis, K., Cok, L, Faldini, R., 2012. DP upgrade after vessel refitting. *10<sup>th</sup> International conference on hydrodynamics ICHD 2012*, 1-4 October, St. Petersburg, Russia.
- [25] Nabergoj, R. Prpic-Orsic, J., Kolacio, I., 2009. Ship-Pipe Interaction during Laying operations. *13<sup>th</sup> Congress International Maritime Association of Mediterranean- IMAM 2009*, 12-15 October, Istanbul, Turkey.
- [26] Ardavanis, K., Nabergoj, R., Mauro, F., 2022. DP Challenges in ANA Platform Jacket Installation. *Brodogradnja*, 73 (4), 1-11. <https://doi.org/10.21278/brod73401>
- [27] Hammersley, J., Handscomb, D., 1964. *Monte Carlo Methods*. Methuen & Co. LTD. <https://doi.org/10.1007/978-94-009-5819-7>
- [28] Niederreiter, H., 1987. Point sets and sequences with small discrepancy. *Monatshefte fur Mathematik*, 104, 272-337. <https://doi.org/10.1007/BF01294651>